

Structural Performance of Multi-sectional CFST Columns with Double Corrugated Plate



P. A. Azna and Ranjan Abraham

Abstract Single concrete filled steel tube (CFST) members are widely used in building structures and bridges due to their high strength, ductility, toughness, fire resistance [1], energy absorption capacity, fast track construction and low cost, which is due to the composite action between steel tube and core concrete. This study examines structural performance of composite columns comprising of concrete filled steel tubes connected with double corrugated plate. T-shape, C-shape and Z-shaped sections are selected for this study. Non-linear finite element (FE) model was developed using ANSYS 16.1 to study structural performance of these special shaped CFST columns (SCFST). SCFST columns were analysed under axial compression, eccentric and lateral loads. Failure pattern, buckling capacity, strength and stiffness of specimens were investigated.

Keywords SCFST columns · Finite element analysis (FEA) · Double corrugated plate · Eccentricity · Buckling analysis

1 Introduction

Single concrete filled steel tube (CFST) members are widely used in building structures and bridges due to their high strength, ductility, toughness, fast track construction and low-cost, which is due to the composite action between steel tube and its core concrete [2]. Moreover, shuttering is not required during construction, which reduces construction cost and time. These advantages have been widely exploited and led to the extensive use of concrete filled tubular structures [3, 4]. To further

P. A. Azna (✉) · R. Abraham

Department of Civil Engineering, Ilahia College of Engineering and Technology, Mulavoor P.O., Muvattupuzha, Ernakulam, Kerala 686673, India
e-mail: aznapa786@gmail.com

R. Abraham

e-mail: ranjanabraham@icet.ac.in

the development of CFST columns and to promote application of CFST columns in building structures, many scholars have proposed special shaped CFST columns, such as multiple cell special shaped CFST columns [5], special shaped columns fabricated using concrete filled steel tubes [6] and special shaped concrete-filled steel tube columns [7].

Studies have shown that constraining effect of special shaped CFST columns is largely concentrated at their corners and this effect decreases rapidly outside the corner. Material strengths of the steel and concrete are not used to their full advantage in column, since constraining effect of steel plate in middle section of column on core concrete is negligible [3]. To address this issue, many scholars have attempted to optimize various special-shaped CFST columns. Zhang et al. [3] proposed L-shaped column comprising concrete filled steel tube connected by double vertical steel plate filled with concrete (LCFST-D). Xu [8] proposed multi-cell shaped CFST column connected by steel linking plates. It has been shown that special-shaped columns comprising CFST connected by single vertical steel plates cannot meet the requirements of high-rise steel housing construction in terms of bearing capacity and welding transverse stiffeners, complicating their application in rapid industrial construction processes.

In this study, structural performance of T-shape, C-shape and Z-shaped columns comprising concrete filled steel tubes connected with double corrugated plate is assessed. A finite element (FE) model was developed using ANSYS 16.1 to understand structural performance of these special shaped CFST columns (SCFST). Columns were analyzed under axial compression, eccentric and lateral loads. Column limbs were provided with concrete filled steel tubes primarily for withstanding compressive forces. Built-up section offered greater stiffness and were proved to be more advantageous in situations of large load eccentricity and/or high slenderness ratio, as it consisted of multiple column limbs. CFST columns with plate connections have been widely used in large-span structures and bridges. Plate connected CFST members could be used as such, as they could be embedded in walls of buildings.

2 Finite Element Modelling

2.1 General

Finite element model was developed using SOLID186 element of ANSYS 16.1 to investigate structural behaviour of SCFST columns. SOLID186 is a higher order 3D 20-node solid element exhibiting quadratic displacement behavior, defined by 20 nodes having three degrees of freedom per node (translations in the nodal x, y and z-directions) ie, UX, UY, UZ.

2.2 Geometry

SCFST column connected with double corrugated plate were adopted for Finite Element Analysis. Sectional dimensions of mono-steel tubes were $100 \times 100 \times 5.75$ mm. Length of column was 3000 mm. Vertical steel plates were provided with a width of 140 mm and thickness of 6 mm. Geometry of T-shape, C-shape and Z-shaped CFST column connected with double corrugated plate in finite Element modelling are shown in Figs. 1 and 2. Mechanical properties of mono-steel tube and vertical steel plate are shown in Table 1. Multilinear isotropic hardening was used to reproduce plastic behavior of materials. Weight of finite element models were kept constant in all cases. Stress–strain curve for steel and concrete are shown in Figs. 3 and 4 respectively.

Figure 5 Boundary conditions of SCFST column with double corrugated plate connection. To simulate real conditions, SCFST column was analyzed with both ends constrained in X, Y, and Z displacement directions. In addition, rotation about

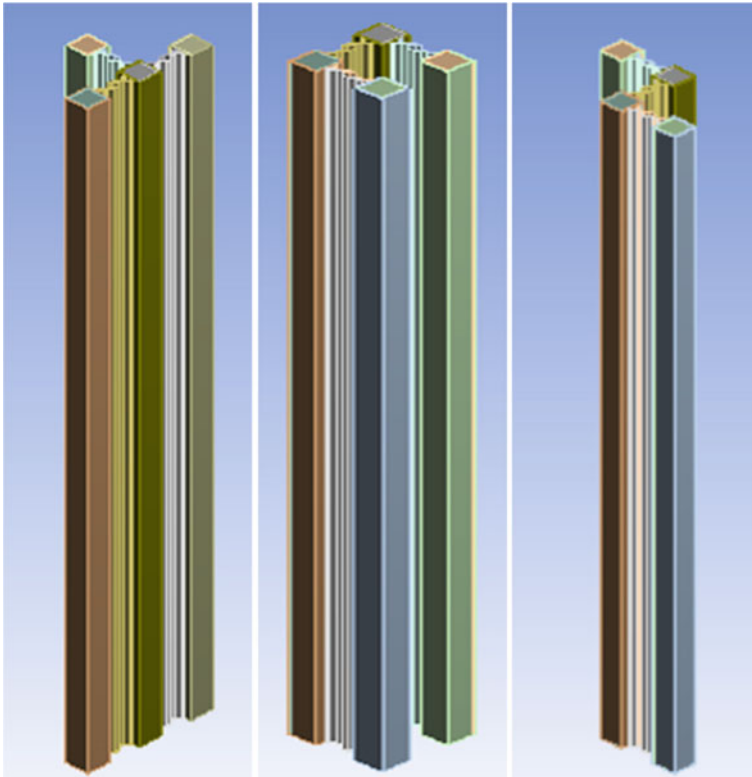


Fig. 1 Geometry of T-shape, C-shape and Z-shaped CFST columns connected with corrugated plate

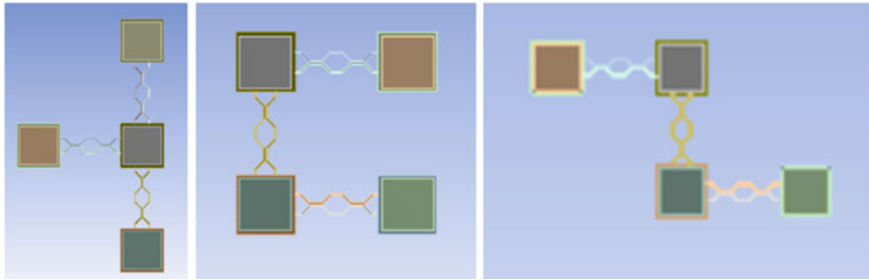


Fig. 2 Top view of T-shape, C-shape and Z-shaped CFST columns connected with corrugated plate

Table 1 Mechanical properties (as in journal [3])

Material	Size or thickness (mm)	f_y (MPa)	E_s (MPa)	Poisson's ratio (μ)
Steel tube	100 × 100 × 5.75	380	2.01×10^5	0.3
Corrugated plate	140 × 6	368	1.76×10^5	0.3
Concrete	$f_c = 32.4 \text{ N/mm}^2$			0.15

f_y = yield strength of steel, E_s = modulus of elasticity of steel, f_c = compressive strength of concrete

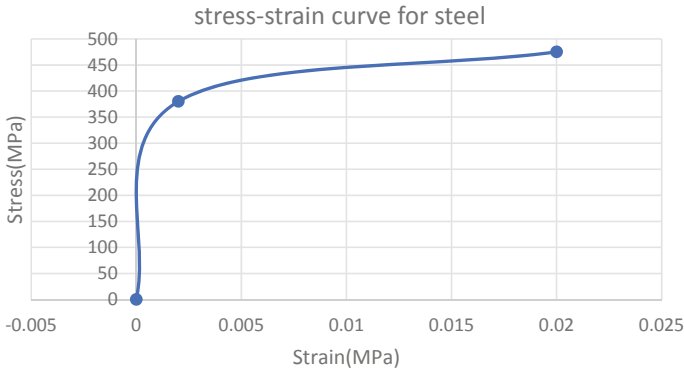


Fig. 3 Stress–strain curve for steel

Y-axis was also constrained and load was applied in one direction. FE contains 3 DOF per node for the model, but support condition is given as remote displacement and it represented in UX, UY, UZ and ROT X, ROT Y, ROT Z. As the support condition is pinned, rotation about y axis was constrained.

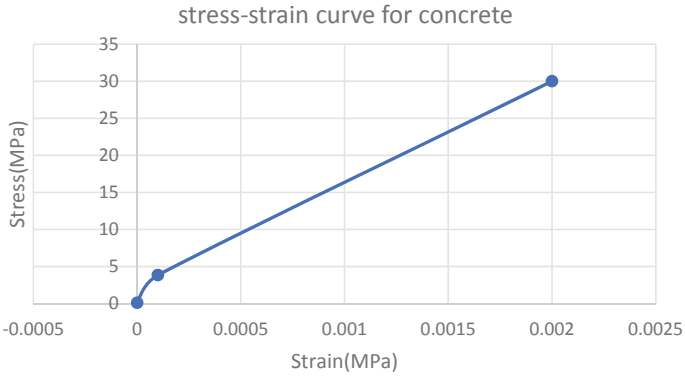


Fig. 4 Stress–strain curve for concrete

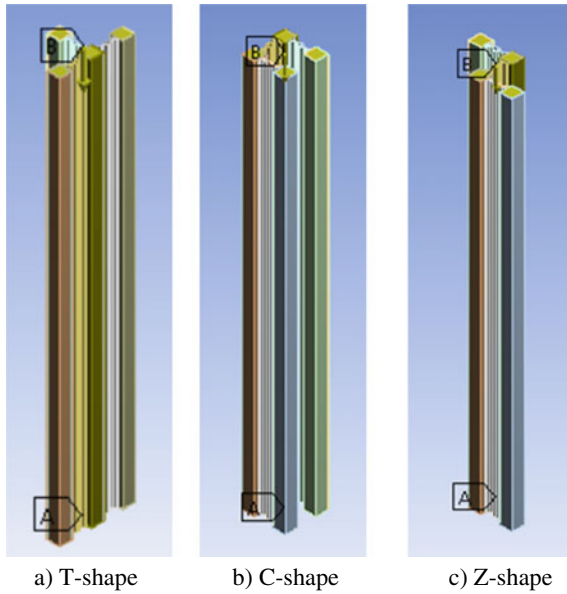


Fig. 5 Boundary conditions of SCFST columns

2.3 Analytical Results

2.3.1 Axial Compression

Columns were axially loaded. Displacement controlled force was given in the analysis. Figure 6 shows comparison of load–displacement curve obtained from finite element model. From load–displacement curve it was observed that, Z-shaped

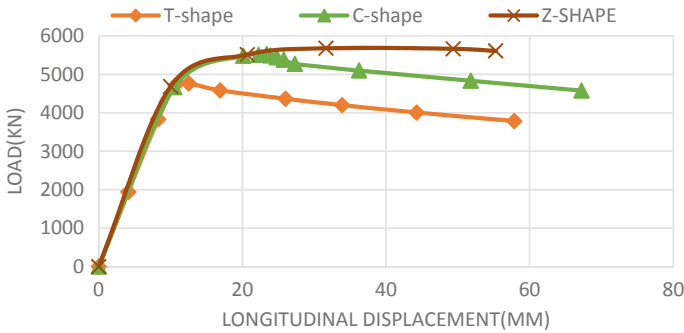


Fig. 6 Comparison of load–displacement curves of specimens

column showed better performance than C-shape and T-shaped column in axial compression. Figure 7 represents stress distribution along entire specimen under axial loading. T-shape and C-shaped column showed complete global buckling towards outside. Global buckling was the major failure mode. Damage occurred mainly in middle part of columns. For Z-shaped column, corner CFST tubes underwent local limb buckling indicating that it resisted lateral deformation and offered better loading performance compared to others.

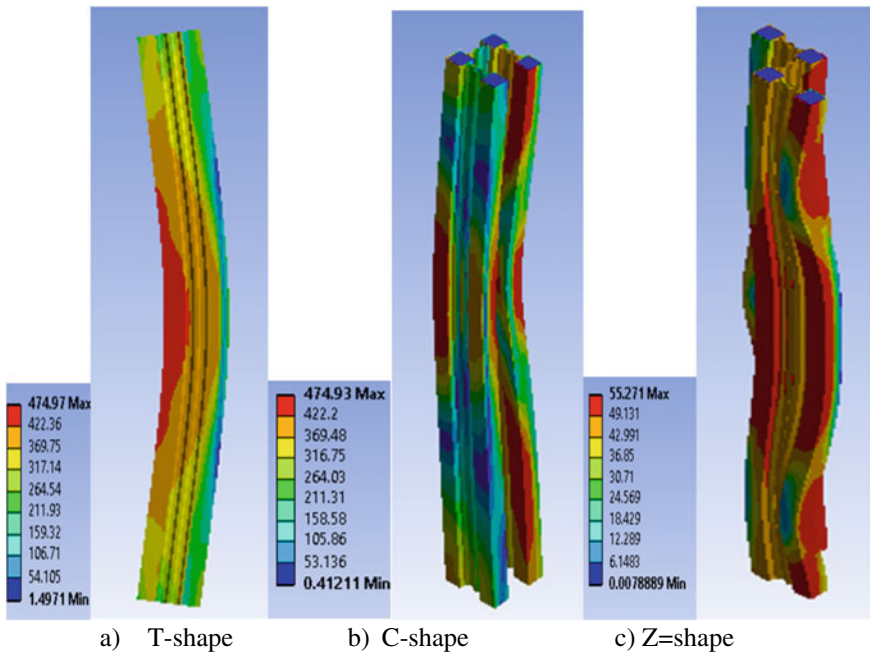


Fig. 7 Von-mises stress diagram of typical failures of specimen

2.3.2 Eccentric Loading

Specimens were analysed for different eccentric loading in both directions. Centroid of composite areas was determined and eccentric loading is given at points of 25% and 50% eccentricity from the CG point. Figures 8 and 9 represents load–displacement comparison of specimens at 25% eccentricity in x and z direction respectively. Table 2 shows the values of eccentricities taken for analysis.

Figure 10 represents variation of ultimate load due to 25% and 50% eccentricity in both X and Z direction. As eccentricity increased, ultimate load reduced. T-shaped column showed better performance under eccentric loading in both directions. Due to asymmetrical shapes, eccentric loading performance in Z-direction was more for C-shape and Z-shaped columns than in X-direction. T-shaped column showed better eccentric performance in X-direction than Z-direction. Figure 11 shows stress variation of specimens and it reveals that each of the specimen largely exhibited global buckling of steel tube towards outside.

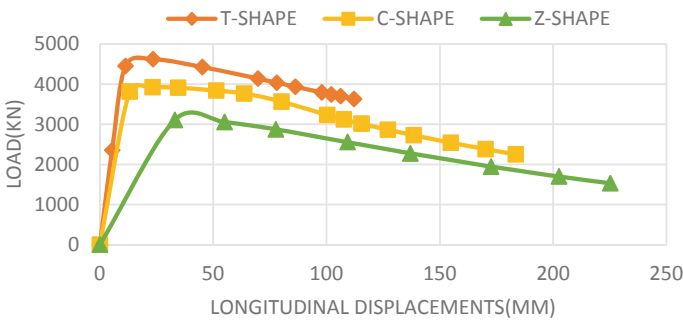


Fig. 8 Comparison of load–displacement curves at an eccentricity of 25% in X-direction

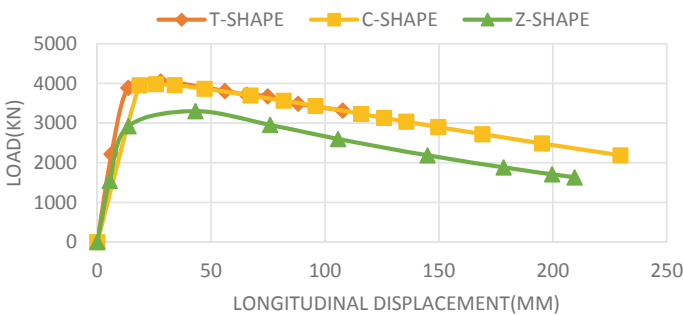


Fig. 9 Comparison of load–displacement curves at an eccentricity of 25% in Z-direction

Table 2 Values of eccentricities taken in both directions

Column type	X-axis		Z-axis	
	25%	50%	25%	50%
T-shape	27.204	54.407	72.5	145
C-shape	42.5	85	42.5	85
Z-shape	72.5	145	42.2	85

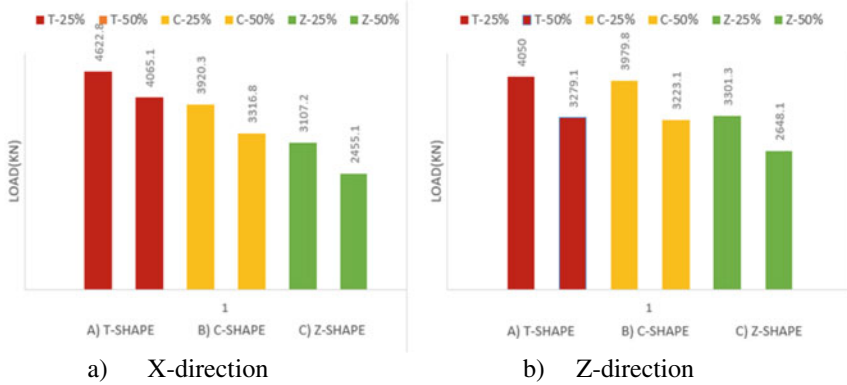


Fig. 10 Comparison of ultimate load at different eccentricity

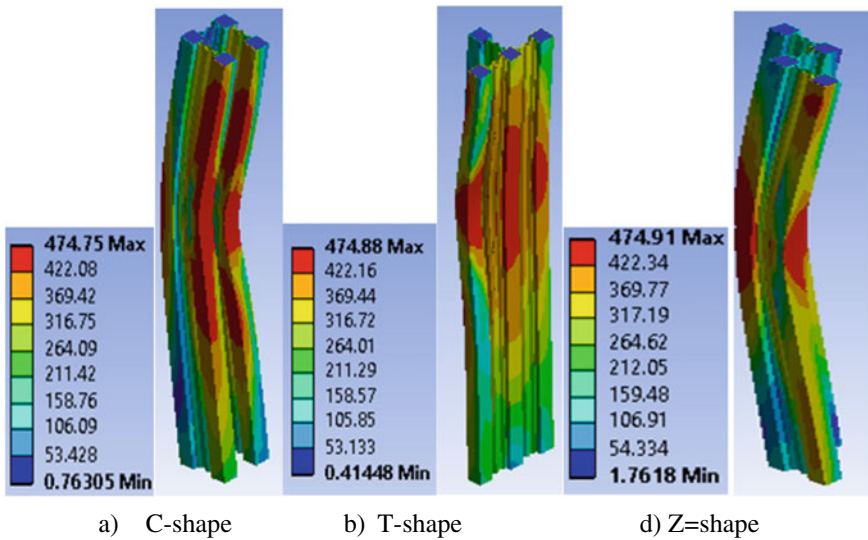


Fig. 11 Von-mises stress diagram of typical failures of specimen

2.3.3 Lateral Loading

Lateral loading is very important in zones of high seismic risk. Lateral loading is achieved by making bottom support fixed and top support free. Based on analysis results, Z-shaped column showed better performance under lateral loading due to stability of its shape rather than ordinary shaped columns. C-shaped column showed more deflection in both x and z direction which means that it has more ductility compared to other ones. Figure 12 represents comparison of lateral load–displacement curves in both x and z direction for each specimen. Deflection was observed to be more for C-shaped column reveals that it is more ductile compared to others.

Z-shaped column showed better performance in both axial and lateral loading conditions and mono columns functioned well together under loading. Table 3 shows results for varying slenderness ratio. Slenderness ratio is checked to show the variation in ultimate strength. As slenderness ratio increased, strength, stiffness and ultimate load decreased and the specimen experienced large deflection. Figure 13 shows variation of ultimate strength due to increase in slenderness ratio under axial loading condition.

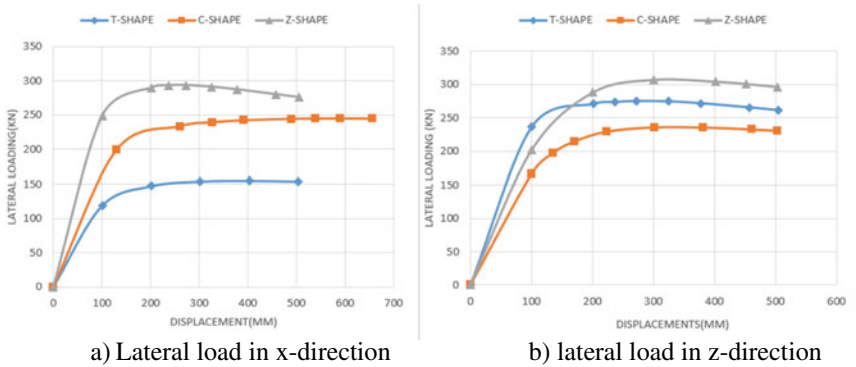


Fig. 12 Comparison of lateral load–displacement curves in x and z-direction

Table 3 Finite element analysis results for varying slenderness ratio

Column type	Size of column (mm)	Length (mm)	Slenderness ratio	Ultimate load (kN)
Z1	100 × 100 × 5.75	2000	16.37	6140
Z2	100 × 100 × 5.75	2500	20.46	6074
Z3	100 × 100 × 5.75	3000	24.55	5678

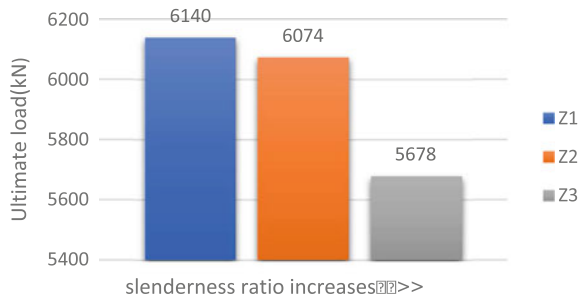


Fig. 13 Variation of strength due to increase in slenderness ratio

2.3.4 Comparison with Hollow Steel Tube Column Under Axial Loading

T-shape, C-shape and Z-shaped hollow steel tubes connected with double corrugated plate were analysed under axial loading for comparing their structural performance with SCFST columns. Figure 14 shows the geometry of hollow steel columns. Figure 16 shows comparison in ultimate strength for SCFST and hollow steel tube columns. Special shaped CFST columns offered better performance than hollow steel tube columns, due to composite action between steel tube and its core concrete. Internal filling with concrete increased load carrying capacity of column and effectively delayed buckling of column due to greater stiffness. Table 4 shows comparison

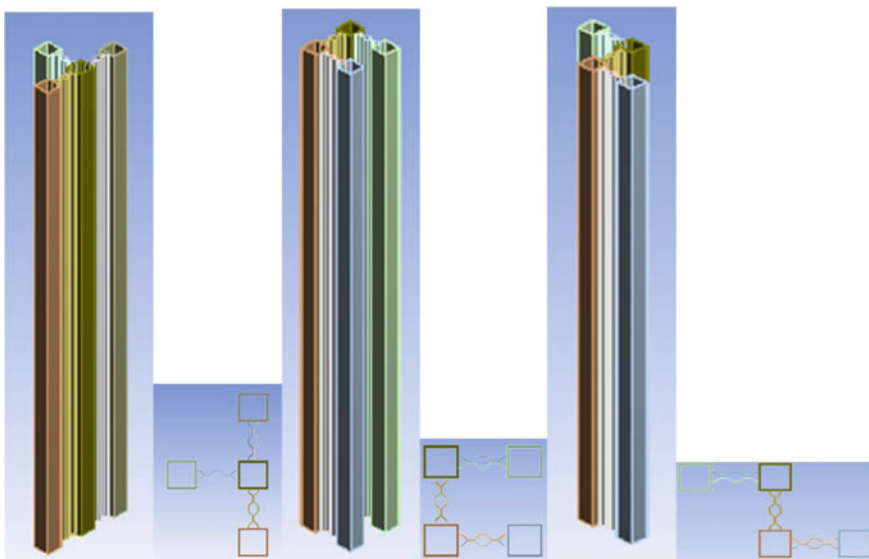


Fig. 14 Geometry of T-shape, C-shape, Z-shape hollow steel tube columns

Table 4 Comparison of load–deflection values

Column type	SCFST		Hollow steel tube	
	Deflection (mm)	Max load (kN)	Deflection (mm)	Max load (kN)
T-shape	12.533	4762.1	16.344	3767.7
C-shape	23.38	5519.5	48.638	5027.6
Z-shape	31.631	5678	46.017	5019.3

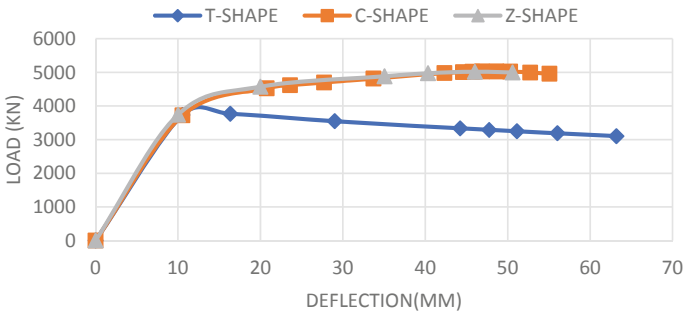


Fig. 15 Comparison of load–displacement curves of specimens

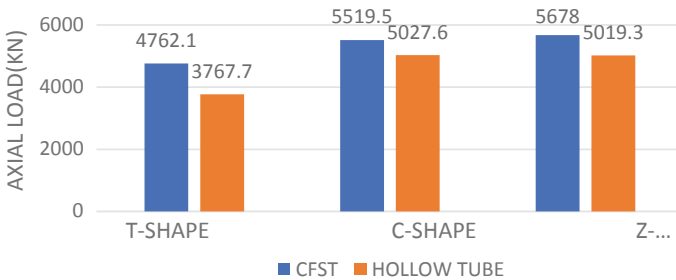


Fig. 16 Comparison of strength for SCFST and hollow steel tubes

of load–deflection values. And Fig. 15 shows the comparison of load–displacement curves.

3 Validation of an LCFST-D Column

The performance of L-shaped columns under axial compression were evaluated by Zhang et al. [3] in the paper—“*Performance of L-shaped columns comprising concrete-filled steel tubes Under axial compression*”. L-shaped CFST column connected by double-vertical steel plate (LCFST-D column) is validated with the data

available in this paper. Finite-element results are compared to the experimental results available from the paper. Table 5 describes the mechanical properties of specimen validated. Figure 17 shows the geometry of LCFST-D column.

The boundary conditions of specimens were set to be same as in the test specified in journal. Coupling points were specified at the centroid of top of the column to form rigid surfaces. Top of the column was constrained in the X and Z displacement directions. Rotation about the X-axis, Y-axis and Z-axis was constrained. Bottom of the column was constrained in the three (X, Y, and Z) displacement directions; in addition, rotation about Y-axis was constrained [3].

Table 5 Mechanical properties of LCFST-D column

Material	Size or thickness (mm)	Length (mm)	f_y (MPa)	E_s (MPa)	Poisson's ratio (μ)
Steel tube	100 × 100 × 5.75	2000	380	2.01×10^5	0.3
Steel plate	100 × 5.75	2000	368	1.76×10^5	0.3
Concrete	$f_c = 32.4 \text{ N/mm}^2$				0.15

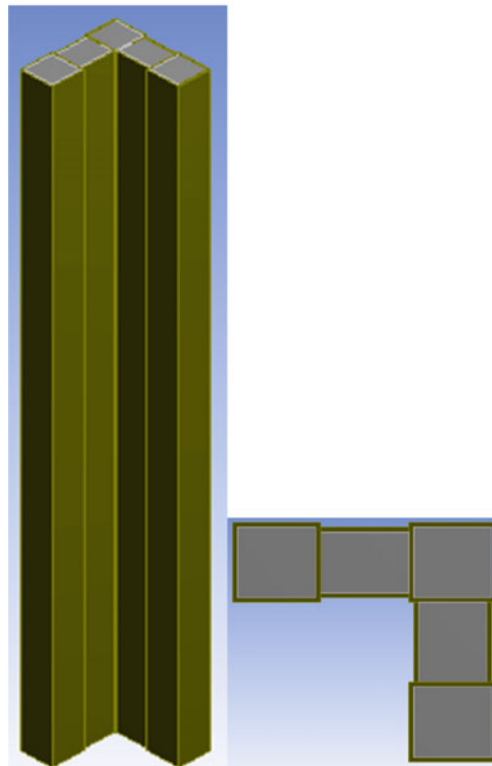


Fig. 17 Geometry of LCFST-D column

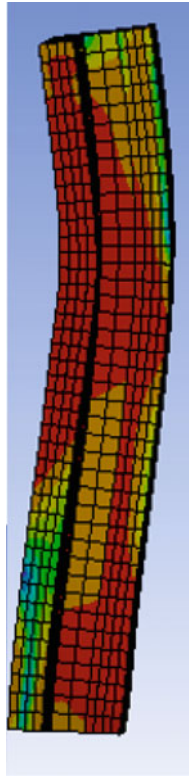


Fig. 18 von-mises stress diagram of failure column

The failure model of finite element simulation was similar to the actual failure model, as shown in Fig. 18. It shows a global buckling behavior. This similarity indicates that finite element model can be used to simulate actual failure. Maximum deformation value from the experimental result obtained is 22.01 mm and total deformation obtained from the finite Element Analysis is 22.25 mm. Figure 19 shows the load–deflection curve of column analyzed. Ultimate load of LCFST-D column analyzed through validation is 4921 kN. The ultimate load of the specimen is about 4603.57 kN from the experimental results and 4958 kN from the finite element results that explained in the journal [3]. Table 6 shows the comparison of results. The percentage of difference in the ultimate load is 6.89% which is within limits.

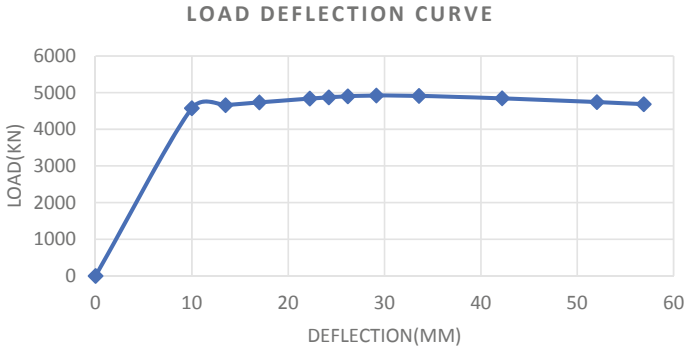


Fig. 19 Load–deflection curve of LCFST-D column

Table 6 Comparison of results

	Ultimate load (kN)	% of error
Experimental	4603.57	6.895138
FEA (validated)	4921	
Journal FEA	4958	

4 Conclusions

Structural performance of SCFST columns under various loading conditions was investigated. Based on results, following conclusions are drawn:

- Global buckling was the major failure mode and damage occurred mainly in middle part of columns and stress was concentrated on outer mono tubes.
- T-shape and C-shaped columns exhibited global buckling of steel tube and vertical corrugated plate towards outside.
- Local limb buckling occurred for Z-shaped column under axial loading and it had less lateral deformation. Local buckling occurred only for end CFST tubes and clear local buckling occurred at top and bottom of corner CFST tube.
- Z-shaped CFST column showed better performance under axial and lateral loads and T-shaped column showed better performance under eccentric load.
- C-shaped column showed more deflection in both x and z direction under lateral loading which means that it has more ductility compared to other ones.
- Slenderness ratio significantly influenced bearing capacity. Ultimate bearing capacity and stiffness of column reduced as slenderness ratio increased.
- SCFST columns showed greater load carrying capacity and stiffness compared to hollow steel tube column.

References

1. Han L-H, Song T-Y, Zhou K, Cui Z-Q (2018) Fire performance of CFST triple-limb laced columns. *J Struct Eng*
2. Yang Y-F, Liu M, Fu F (2018) Experimental and numerical investigation on the performance of three-legged CFST latticed columns under lateral cyclic loadings. *J Thin-Walled Struct* 132:176–194
3. Zhang W, Chen Z, Xiong Q (2018) Performance of L-shaped columns comprising concrete filled steel tubes under axial compression. *J Constr Steel Res* 145:573–590
4. Huang Z, Jiang L-Z, Frank Chen Y, Luo Y, Zhou W-B (2018) Experimental study on the seismic performance of concrete filled steel tubular laced columns. *J Steel Compos Struct* 26(6):719–731
5. Yang Y, Yang H, Zhang S (2010) Compressive behaviour of T-shaped concrete filled steel tubular columns. *Int J Steel Struct* 10(4):419–430
6. Chen Z, Bin R, Fafitis AS (2009) Axial compression stability of a crisscross section column composed of concrete-filled square steel tubes. *J Mech Mater Struct* 4(10)
7. Tao Z, Wang ZB, Yu Q (2013) Finite element modelling of concrete filled steel-tub columns under axial compression. *J Constr Steel Res* 89(5):121–131
8. Xu M, Zhoua T, Chena Z, Li Y, Bisby L (2016) Experimental study of slender LCFST columns connected by steel linking plates. *J Constr Steel Res* 127:231–241